

# Chiral symmetry and spectral properties of the Dirac operator in $G_2$ Yang-Mills Theory

Julia Danzer, Christof Gattringer and Axel Maas

Institute for Physics, Universitätsplatz 5, Karl-Franzens University Graz  
A-8010 Graz, Austria

## Abstract

We study spontaneous chiral symmetry breaking and the spectral properties of the staggered lattice Dirac operator using quenched gauge configurations for the exceptional group  $G_2$ , which has a trivial center. In particular we study the system below and above the finite temperature transition and use the temporal boundary conditions of the fermions to probe the system. We evaluate several observables: The spectral density at the origin, the spectral gap, the chiral condensate and the recently proposed dual chiral condensate. We show that chiral symmetry is broken at low temperatures and is restored at high temperatures at the thermodynamic phase transition. Concerning the role of the boundary conditions we establish that in all respects the spectral quantities behave for  $G_2$  in exactly the same way as for  $SU(N)$ , when for the latter group the gauge ensemble above  $T_c$  is restricted to the sector of configurations with real Polyakov loop.

## Introductory remarks

Confinement of quarks and the breaking of chiral symmetry are two of the key features of QCD. As the temperature is increased, QCD changes its behavior: Quarks become deconfined and chiral symmetry is restored. It is a long standing question whether the two phenomena and their changing behavior at the QCD finite temperature phase transition are linked by some underlying mechanism.

The gauge groups usually considered in Yang-Mills theories are  $SU(N)$ , in particular  $SU(3)$ . These groups have the non-trivial center groups  $\mathbb{Z}_N$  (and  $\mathbb{Z}_3$ , respectively). It has been speculated that the center degrees of freedom play an important role for confinement (see [1] and references therein), as well as for chiral symmetry breaking [2].

However, once dynamical fermions in the fundamental representation are introduced, the center is explicitly broken, and confinement is no longer signaled by an infinitely rising potential. Nonetheless, the chiral transition and the transition manifest in residual center observables still coincide.

On the other hand, when the quarks are in the adjoint representation [3], the center symmetry is still intact at low temperatures, and the finite temperature transition is signaled by a change of center-sensitive observables, like the Polyakov loop, without affecting qualitatively the breaking of chiral symmetry. Only at much larger temperature chiral symmetry becomes restored.

In order to understand better the role of the center degrees of freedom for confinement, in a series of papers [4] – [9] lattice QCD has been studied for the gauge group  $G_2$  where the center is trivial, i.e., consists of only the identity element. These papers were all motivated by understanding various aspects of confinement. This is due to the fact that  $G_2$  Yang-Mills theory has a place in between Yang-Mills theory, adjoint QCD and full QCD: It exhibits a linear rising potential with Casimir scaling [9], which, however, flattens out at large distances [4], as is the case in full QCD. Its bound state spectrum resembles adjoint QCD, as gluons can screen quarks and thus permit color-neutral quark-gluon bound states in addition to glueballs and hadrons [4]. Finally, it exhibits a first order phase transition, as does  $SU(N)$  Yang-Mills theory [5, 6, 7]. Furthermore, gluonic correlators seem not to differ qualitatively from the  $SU(N)$  case [8].

So far, however, essentially nothing is known about aspects of chiral symmetry and its breaking for a center-trivial gauge group. In particular, due to its intermediate status between the other three types of theory, it is a-priori unclear whether chiral symmetry breaking is present at all at low temperature, or, if chiral symmetry is broken, whether the chiral phase transition coincides with the thermodynamic one.

In our exploratory study we address for the quenched case the questions:

- Is chiral symmetry broken in the confining phase? (Yes!)
- Is chiral symmetry restored at high temperatures? (Yes!)
- Does chiral symmetry restoration take place at the same temperature where the theory deconfines? (Yes!)
- How do the temporal boundary conditions of the Dirac operator influence the spectral quantities and thus observables for chiral symmetry?

These questions can be formulated and answered in terms of spectral quantities of the Dirac operator, in particular the density of eigenvalues near the origin or a possible spectral gap, which appears above the critical temperature  $T_c$ . In our paper we analyze spectral properties of the staggered lattice Dirac operator using quenched  $G_2$  gauge configurations below and above  $T_c$ .

## The role of temporal fermionic boundary conditions in $SU(N)$

When QCD at finite temperature is considered in the Euclidean path integral formalism the time extent of space-time is finite. In such a setting the temporal boundary conditions become a relevant issue. During recent years the role of the temporal fermion boundary conditions was analyzed in several lattice QCD studies [10] – [23]. A part of these studies [10, 11, 12, 13, 14] was motivated by analyzing caloron and dyon signatures of the QCD vacuum, where for the case of calorons [24] specific signatures of Dirac eigenmodes for different boundary conditions are known [25]. Another motivation was a possible persistence of the chiral condensate above  $T_c$  [15, 16, 17, 18, 19], and more recently the temporal fermion boundary conditions were used to relate observables for chiral symmetry to observables for center symmetry [20, 21, 22, 23].

Although the motivations of the studies [10] – [23] are different, one may infer two common observations which are of interest for the present paper:

1. Below the critical temperature  $T_c$  spectral quantities of the Dirac operator are insensitive to the temporal boundary condition.
2. Above  $T_c$  spectral quantities feel the boundary conditions, but only the boundary angle relative to the phase of the Polyakov loop is relevant.

Let us be a little bit more explicit on the second observation. The temporal fermionic boundary condition may be parameterized by an angle  $\varphi \in [-\pi, \pi)$  such that it reads

$$\psi(\vec{x}, \beta) = e^{i\varphi} \psi(\vec{x}, 0) . \quad (1)$$

In this equation  $\beta$  denotes the extent of the Euclidean time direction, i.e., the inverse temperature (in lattice units). It is obvious, that the choice  $\varphi = \pi$  gives rise to the usual anti-periodic boundary conditions. Here, however, we allow for more general boundary conditions and use the angle  $\varphi$  as a free parameter to probe the system.

The second relevant angle in the above listed observation is the phase  $\theta_P$  of the (space-averaged) Polyakov loop

$$P = \frac{1}{V_3} \sum_{\vec{x}} \text{Tr} \prod_{x_4=1}^{\beta} U_4(\vec{x}, x_4) . \quad (2)$$

In the quenched theory below  $T_c$  the expectation value of  $P$  vanishes, while above the transition a non-vanishing expectation value emerges. For the case of the gauge group  $SU(N)$ , the values for the Polyakov loop phases  $\theta_P$  scatter around the phases of the center  $\mathbb{Z}_N$  of  $SU(N)$ , i.e.,  $\theta_P \sim n2\pi/N, n = 0, 1, \dots, N - 1$ . Only for infinite volume the underlying center symmetry of the theory becomes broken and the Polyakov loop assumes a fixed phase  $\theta_P$  of one of the center values. These properties of  $P$  are illustrated in the lhs. plot of Fig. 1 for the case of  $SU(3)$ , where we show a scatter plot of the Polyakov loop values in the complex plane for two ensembles below and above  $T_c$ . It is obvious that above  $T_c$  the phases scatter around the values  $0, 2\pi/3$  and  $4\pi/3$ . The subsets of configurations where the Polyakov loop assumes a single one of the possible phases will be referred to as *Polyakov loop sectors*. In particular we will call the set of configurations where the Polyakov loop is essentially real, i.e.,  $\theta_P \sim 0$ , the *real Polyakov loop sector*.

The second observation from the list above can now be formulated precisely: Only the sum  $\sigma$  of the boundary angle  $\varphi$  and the phase  $\theta_P$  of the Polyakov loop,

$$\sigma = \varphi + \theta_P \text{ mod } 2\pi , \quad (3)$$

is relevant for spectral observables of the Dirac operator. In other words, the change of observables found when switching from one center sector of the Polyakov loop to another one can be compensated by shifting the fermionic boundary conditions. This has been observed [10] – [23] in the gauge groups  $SU(2)$  and  $SU(3)$  for a wide range of quantities, ranging from the spectral gap to localization properties of zero and near-zero modes.

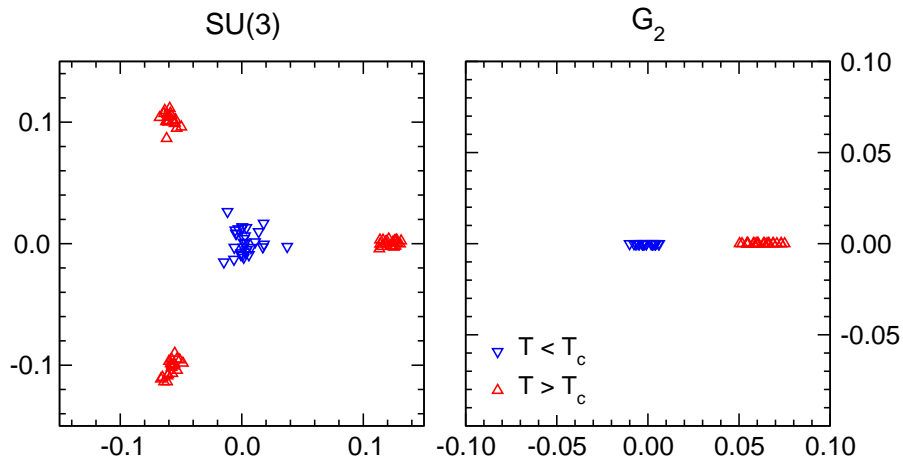


Figure 1: Scatter plots of the Polyakov loop  $P$  in the complex plane for gauge configurations below and above  $T_c$ . The lhs. plot is for gauge group  $SU(3)$ , while the rhs. shows the case of  $G_2$ .

In its most compact form the results for the spectrum may be written down as a generalization [21] of the well known Banks-Casher formula [26]. This formula relates the chiral condensate  $\langle \bar{\psi}\psi \rangle$  to the density  $\rho(0)$  of the Dirac eigenvalues at the origin,

$$\langle \bar{\psi}\psi \rangle_\sigma = -\pi \rho(0)_\sigma. \quad (4)$$

We attach the subscript  $\sigma$  to denote the total angle, consisting of the Polyakov loop phase and the boundary angle used for the evaluation of the two sides.

Below  $T_c$  the spectrum extends all the way to the origin and a non-vanishing  $\rho(0)$  exists which is independent of  $\sigma$ . Thus  $\langle \bar{\psi}\psi \rangle \neq 0$  and chiral symmetry is broken. Above  $T_c$  a gap is expected to open up in the spectrum such that  $\rho(0)$  vanishes and chiral symmetry is restored ( $\langle \bar{\psi}\psi \rangle = 0$ ).

The interesting observation is that for a zero total angle  $\sigma = 0$  a non-vanishing density of eigenvalues  $\rho(0)$  and thus a non-zero chiral condensate persists also above  $T_c$ . Such a zero total angle  $\sigma = 0$  is, e.g., obtained when periodic boundary conditions ( $\varphi = 0$ ) are used in the real Polyakov loop sector ( $\theta_P = 0$ ). Another possibility for  $\sigma = 0$  would be anti-periodic boundary conditions for a Polyakov loop with phase  $\theta_P = \pi$ , which is possible for gauge group  $SU(N)$  with even  $N$ . More generally it may be shown [12] that the spectral gap has a sine-like dependence on  $\sigma$  and thus closes completely at  $\sigma = 0$ .

Having identified the role of the center  $\mathbb{Z}_N$  of the gauge groups  $SU(N)$  and the corresponding phase sectors of the Polyakov loop for the spectral quantities, an interesting question comes up: How do spectral quantities, and thus the chiral condensate below and above  $T_c$ , behave when the gauge group has a trivial center, i.e., the center consists of only the identity element, as is the case for the group  $G_2$ ? And how do the fermionic temporal boundary conditions influence the Dirac spectrum in this case?

Before we address these questions in the next sections, we conclude with remarking that also for the case of  $G_2$  the finite temperature transition is signaled by a changing expectation value of the Polyakov loop [5]. Below  $T_c$  this expectation value is zero, while at  $T_c$  it jumps in a first order transition<sup>1</sup> to a non-vanishing value. This behavior is illustrated in the rhs. plot of Fig. 1 (see also Fig. 2 below), where we again show scatter plots of the Polyakov loop values below and above  $T_c$ , now for gauge group  $G_2$ . What is immediately obvious is the fact that the Polyakov values are real, due to the existence of real representations of  $G_2$ .

Furthermore, above  $T_c$  no non-trivial phase structure appears. However, in the infinite volume limit the Polyakov loop in both phases will necessarily vanish, since there is no asymptotic string tension [5]. The phase transition is nonetheless physical, as it is manifest also in the free energy [5, 7].

## The setting of our calculation

### Technicalities

For our simulations we used the standard Wilson action with the links in a fundamental, but complex, 7-dimensional representation [5, 6].

For our analysis we use quenched  $G_2$  configurations at finite temperatures below and above the critical temperature. We worked with different lattice sizes ranging from  $8^3 \times 4$  to  $14^3 \times 6$ , and  $\beta$  values between 9.45 and 10. All results we show are for lattice size  $12^3 \times 6$ . The configurations are generated with a hybrid heat-bath [5, 6] and overrelaxation [8] algorithm. Details can be found in [8]. We always made several independent runs to reduce autocorrelation effects, with no more than ten configurations per run generated for fermionic observables. We allowed for 28 to 34 thermalization sweeps and between 80 to 140 decorrelation sweeps between consecutive measurements.

---

<sup>1</sup>This transition should not be confused with the bulk transition [5, 6] at a lower inverse coupling,  $\beta = 9.45$ , which is, however, irrelevant for all considerations here.

For scale setting we use the string tension determined from Wilson loops<sup>2</sup> [9]. In some of our plots we use units of GeV for illustration purposes. These were introduced by using for the  $G_2$  string tension the value known for  $SU(3)$  ( $\sigma = (0.44 \text{ GeV})^2$ ). Note that since even quenched  $G_2$  Yang-Mills theory does not exhibit an asymptotic linear rising potential, the intermediate distance string-tension has been used to fix the scale. Intermediate distance is here the distance where Casimir scaling of the string tension is observed [9]. At larger distances the potential flattens out in quenched  $G_2$ , while it becomes  $N$ -ality scaling in  $SU(N)$  Yang-Mills theory. Note that this is nonetheless equivalent to the procedure to set the scale in full QCD, as also there in the Casimir-region the scale is fixed. The critical coupling  $\beta_c$ , and thus temperature  $T_c$ , was taken from [7], but we also observed them by Polyakov-loop and plaquette observables, reproducing the results of [7].

The fermionic observables computed from complete Dirac operator spectra were evaluated on typically 40 configurations at each temperature. The error bars we show are statistical errors determined from single elimination Jackknife.

For the analysis of the fermionic variables we use the staggered lattice Dirac operator

$$D_{xy} = \sum_{\mu=1}^4 \frac{\eta_{\mu}(x)}{2a} [U_{\mu}(x)\delta_{x+\hat{\mu},y} - U_{\mu}(x-\hat{\mu})^{\dagger}\delta_{x-\hat{\mu},y}], \quad (5)$$

with the staggered sign function  $\eta_{\mu}(x) = (-1)^{x_1 + \dots + x_{\mu-1}}$ . The coordinates  $x, y$  run over all sites of the 4-dimensional  $L^3 \times N_4$  lattice. The gauge link variables  $U_{\mu}(x)$  are elements of the gauge group  $G_2$ . The staggered Dirac operator is an anti-Hermitian matrix and has its eigenvalues on the imaginary axis. We evaluate complete spectra using a parallel implementation of standard LAPACK routines. For each ensemble the complete spectra were computed for several different fermionic temporal boundary conditions (1). These are most simply implemented by attaching the phase to the last temporal link of the lattice. All the fermionic observables which we discuss below (eigenvalue density, chiral condensate, spectral gap and the dual chiral condensate) may be computed from the spectra at the different boundary conditions.

---

<sup>2</sup>We thank Ludovit Liptak for providing us with his results, partly unpublished, of a high precision determination of the scale.

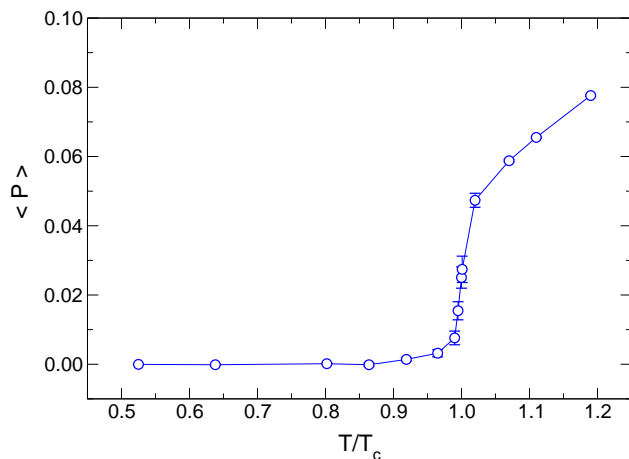


Figure 2: Expectation value of the Polyakov loop as function of temperature.

### Gluonic observables

For illustration purposes we briefly discuss the results for the Polyakov loop. In particular the plot of the Polyakov loop as a function of the temperature will later be useful for comparison when we present our results for fermionic observables as a function of the temperature.

In Fig. 2 we show our results for the Polyakov loop as a function of the temperature on a  $12^3 \times 6$  lattice. The plot clearly shows a steep rise of the expectation value of the Polyakov loop at the critical temperature  $T_c$ .

The transition at the critical temperature is known to be of first order [5, 7]. This is also clearly seen in our ensembles as is demonstrated in Fig. 3, where we show for the  $12^3 \times 6$  lattice histograms of the Polyakov loop at  $T < T_c$  (lhs. plot),  $T = T_c$  (center) and  $T > T_c$  (rhs. plot). The double peak structure in the center plot clearly shows the coexistence of two phases at the critical temperature, thus indicating the first order transition. This result can also be deduced from the free energy [7].

This similarity of gluonic observables for  $G_2$  and  $SU(N)$  gauge theories was discussed previously in the context of confinement [4, 27], and it was conjectured that gluonic observables should coincide qualitatively in both cases [27].



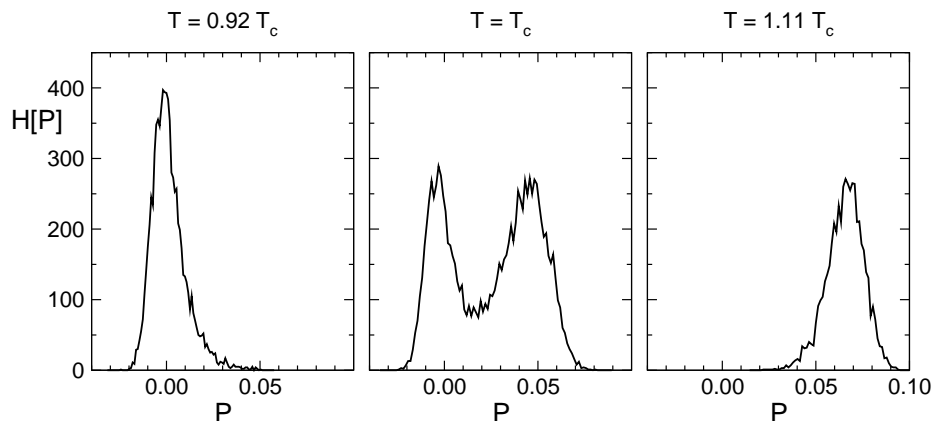


Figure 3: Histograms for the values of the Polyakov loop  $P$ . We compare three temperatures below (lhs. plot), at (center) and above  $T_c$  (rhs. plot). Similar observations have been made in [5].

## Dirac spectra and fermionic observables

### Spectral density at the origin and the chiral condensate

As we have discussed above, the eigenvalue density of the Dirac operator near the origin is related to the chiral condensate via the Banks-Casher relation (4). For the case of  $SU(N)$  gauge theories we know that the spectrum behaves differently for different boundary conditions. In particular for the gauge ensemble restricted to configurations with Polyakov loop in the real sector, the density vanishes above  $T_c$  for all boundary conditions, except for the case where the fermionic boundary condition in time direction is chosen periodic. For the other sectors of the Polyakov loop, the condensate persists for accordingly shifted boundary angles  $\varphi = 2\pi(N-1)/N, \varphi = 2\pi(N-2)/N \dots$ .

For the gauge group  $G_2$  the Polyakov loop is always real and in order to test if this case is similar to  $SU(N)$  we need to compare periodic and anti-periodic temporal fermion boundary conditions. In Fig. 4 we show histograms of the eigenvalues near the origin for several temperatures below and above  $T_c$ . The top panel of plots is for anti-periodic boundary conditions, while at the bottom we show the periodic case.

For the anti-periodic case we find that below  $T_c$  the eigenvalue density extends all the way to the origin. At  $T_c$  it starts to drop and vanishes above the critical temperature. For the periodic boundary conditions the situation is

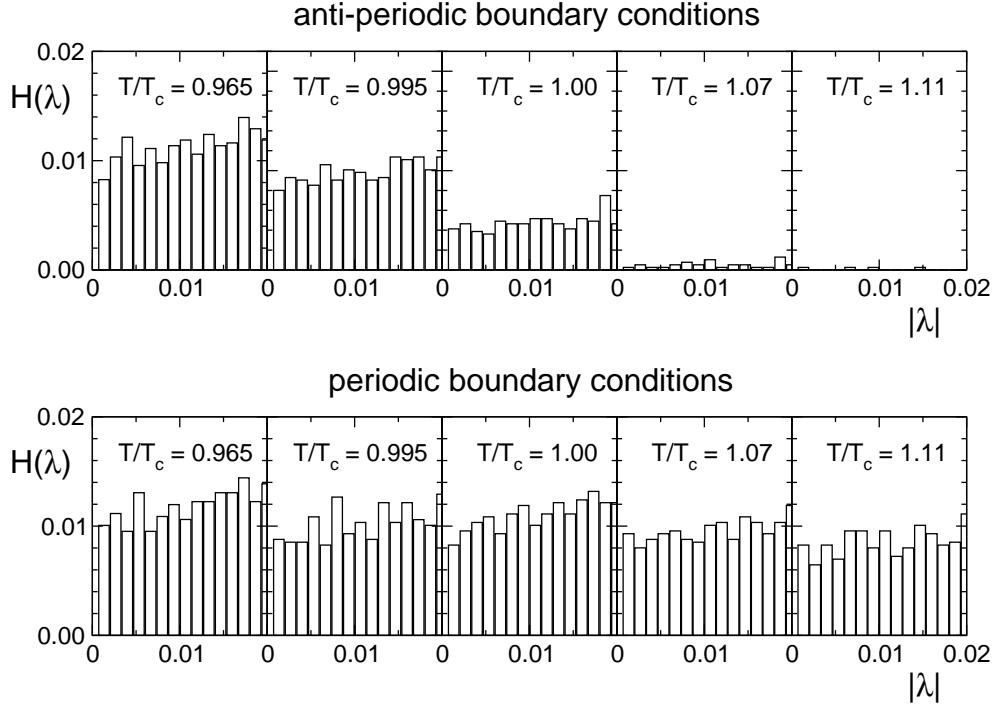


Figure 4: Distribution of the Dirac eigenvalues  $\lambda$  as a function of  $|\lambda|$ . We show the distribution for several values of the temperature below and above  $T_c$  and compare anti-periodic (top panel) to periodic (bottom) boundary conditions.

different, and the density at the origin survives also above  $T_c$ . The histograms clearly demonstrate that the spectral density behaves similar to what was found for  $SU(N)$  when the real Polyakov loop sector is selected.

Since the spectral density at the origin and the chiral condensate  $\langle \bar{\psi}\psi \rangle$  are linked through the Banks-Casher formula (4), it is natural to now study the condensate as a function of the temperature for periodic and anti-periodic boundary conditions.

In our analysis of the condensate we compared two different ways for its determination. First we computed  $\langle \bar{\psi}\psi \rangle$  from the density near the origin as determined from the histograms. Our second determination was based on a direct evaluation of the condensate at a finite fermion mass  $m$ , which is computed as

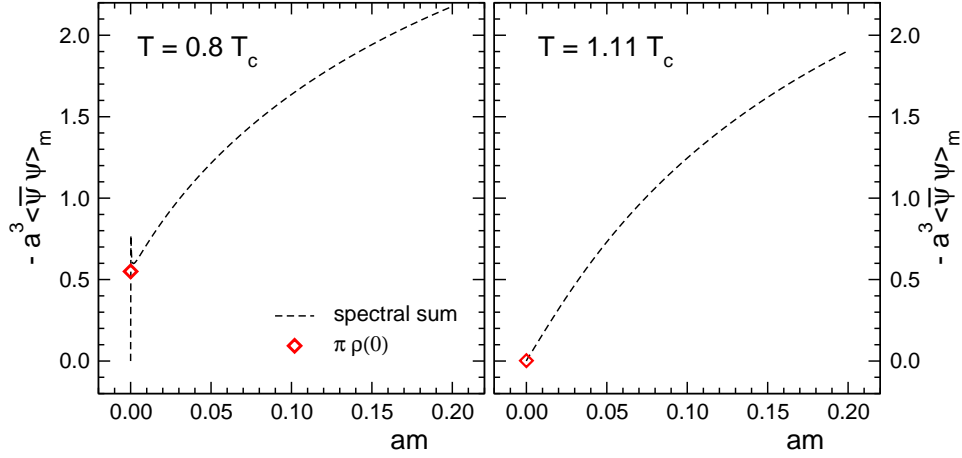


Figure 5: The condensate  $\langle \bar{\psi} \psi \rangle_m$  as a function of the quark mass (dashed curve) compared to the result for the chiral condensate as obtained from the spectral density method (symbols). All quantities are in lattice units and were obtained on our  $12^3 \times 4$  configurations. We compare  $T = 0.8T_c$  (lhs. plot) to  $T = 1.11T_c$  (rhs. plot).

a spectral sum of the Dirac eigenvalues  $\lambda_i$ :

$$\langle \bar{\psi} \psi \rangle_m = -\frac{1}{V} \sum_i \frac{1}{\lambda_i + m}. \quad (6)$$

The proper chiral condensate is obtained by performing the limit  $m \rightarrow 0$  after the infinite volume limit  $V \rightarrow \infty$  is taken. On a finite volume, as one is restricted to in a numerical analysis, the condensate must vanish exactly, as no spontaneous symmetry breaking is possible in a finite system. This is clearly seen in our data for  $\langle \bar{\psi} \psi \rangle_m$  which vanish for very small  $m$ . However, before vanishing completely,  $\langle \bar{\psi} \psi \rangle_m$  shows a long and pronounced shoulder which may be extrapolated to vanishing mass. Comparing the results from this extrapolation to the determination from the spectral density we always found the discrepancies to be in the one percent range, showing that the two methods give the same result.

We demonstrate this agreement explicitly in Fig. 5, where we show the result from the spectral sum (6) as a function of the mass parameter (dashed curve) and compare it to the outcome from the spectral density method (symbol). We show the results for  $T = 0.8T_c$  where the condensate is finite (lhs. plot) and for  $T = 1.11T_c$  (rhs.) where the condensate vanishes (using anti-periodic temporal

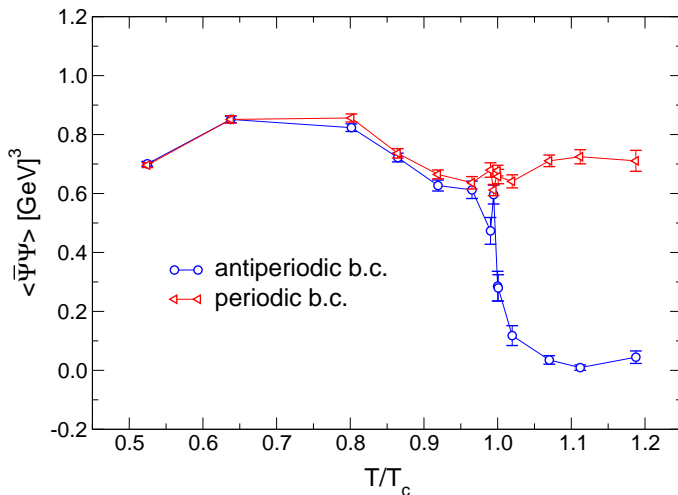


Figure 6: The chiral condensate as a function of the temperature. We compare the results for anti-periodic temporal boundary conditions to the case of periodic boundary conditions.

boundary conditions in both cases). The lhs. plot shows the described shoulder-type behavior, before it drops to zero at vanishing mass. Just before this drop we observe a small spike which is due to isolated small eigenmodes on individual configurations – an observation we made for some of our ensembles. When one ignores this spike and extrapolates the shoulder to vanishing quark mass, one ends up exactly on the spectral density result indicated by the symbol. On the rhs. plot no shoulder is observed and the condensate directly extrapolates to zero in agreement with the spectral method for that case.

The results for the chiral condensate as a function of the temperature are shown in Fig. 6, where we again compare periodic and anti-periodic boundary conditions. As was already suggested by the histograms in Fig. 4, only the anti-periodic case shows a restoration of chiral symmetry, i.e., a condensate that vanishes above  $T_c$ . For the periodic case, where the boundary condition is in phase with the Polyakov loop, we see that the condensate persists also above  $T_c$ . Again we find the same picture as for  $SU(N)$  gauge theory in the real Polyakov loop sector.

Let us finally stress that the fact that the condensate for anti-periodic boundary conditions drops at the same critical temperature  $T_c$  where also the Polyakov loop and the free energy indicate the transition (compare Fig. 2), is in itself a remarkable finding. One cannot a priori expect that this is the case, as is known

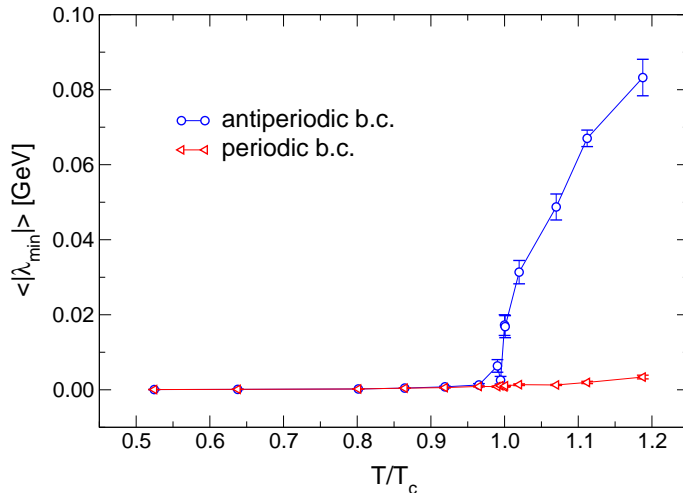


Figure 7: The spectral gap as a function of the temperature. We compare the results for anti-periodic temporal boundary conditions to the case of periodic boundary conditions.

from the example of  $SU(3)$  with quarks in the adjoint representation [3]. On the other hand it was shown in [20] – [23] that with the help of boundary conditions the chiral condensate may be transformed into a generalized Polyakov loop. This transformation suggests a strong link between chiral symmetry and confinement, although the exception of adjoint quarks coupled to  $SU(3)$  gluons (and likely for  $SU(N)$ ) still needs to be understood in this connection. In particular, it would be highly interesting to investigate whether for adjoint  $G_2$  quarks the transitions would also be distinct and thus would be a general feature of the adjoint representation, or whether this is specific to adjoint  $SU(N)$  fermions.

### The spectral gap

Having obtained the behavior of the chiral condensate let us now look at the spectral gap, i.e., the average size  $\langle |\lambda_{\min}| \rangle$  of the smallest eigenvalue  $\lambda_{\min}$ . Below  $T_c$  the density of eigenvalues extends all the way to the origin, which on a finite lattice gives rise to only a microscopic gap, which is a finite size effect that may be described by random matrix theory. At  $T_c$  a macroscopic gap opens up in the spectrum, such that the density at the origin and thus the condensate vanish. However, as discussed, for  $SU(N)$  the size of the gap depends on the total angle of Polyakov loop and boundary phase.

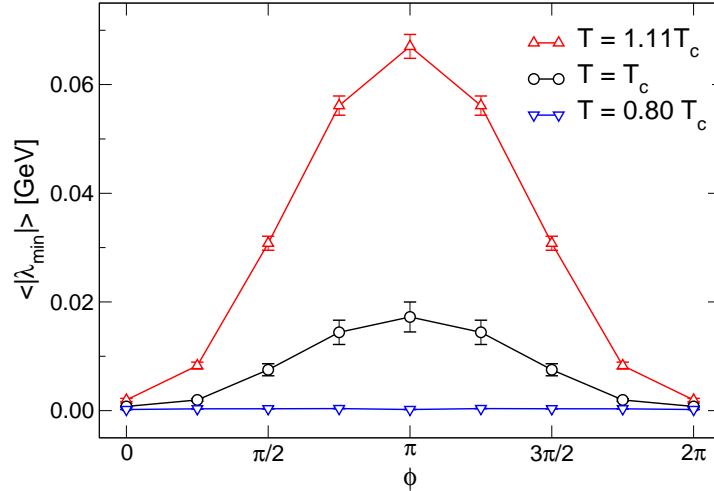


Figure 8: The spectral gap as a function of the boundary angle  $\varphi$ . We compare the data for three different temperatures.

In Fig. 7 we now analyze the spectral gap, i.e.,  $\langle |\lambda_{min}| \rangle$ , as a function of the temperature, comparing periodic and anti-periodic boundary conditions. The plot demonstrates very clearly that the gap opens up only when the anti-periodic boundary conditions are used. For the periodic case, it remains closed. Since the Polyakov loop is real, the vanishing gap for periodic boundary conditions obeys the  $\sigma = 0$  criterion of Eq. (3). Thus also in this respect the gap behaves like in the case of  $SU(N)$ .

To complete the analysis of the spectral gap, in Fig. 8 we plot it as a function of the boundary angle  $\varphi$ , comparing three temperatures. Below  $T_c$  the gap is essentially zero, and the remaining microscopic gap shows no  $\varphi$ -dependence within error bars. At  $T_c$  a slight sine-like behavior becomes visible, which becomes considerably more pronounced above  $T_c$ . Using anti-periodic boundary conditions, i.e.,  $\varphi = \pi$ , one picks up the value of the gap at maximal opening. As is seen in Fig. 7, this maximal gap grows monotonically over the range of temperatures which we studied above  $T_c$ . For periodic boundary conditions, i.e.,  $\varphi = 0 \equiv 2\pi$ , the gap is closed. We stress that this closing is not just visible for the smallest eigenvalue which defines the gap, but as is obvious from the histograms in Fig. 4, also the higher eigenvalues come closer to zero. Thus indeed a finite spectral density and thus a non-vanishing condensate are found above  $T_c$  for periodic boundary conditions, as was already demonstrated in Fig. 6.

## The dual chiral condensate

We finally come to an observable which is based on the non-trivial dependence of spectral quantities above  $T_c$  on the fermionic boundary condition, the recently proposed [21] dual chiral condensate  $\Sigma_1$ . It is obtained as a Fourier transform of the usual chiral condensate with respect to the boundary angle,

$$\Sigma_1 = -\frac{1}{2\pi} \int_{-\pi}^{\pi} d\varphi e^{-i\varphi} \langle \bar{\psi} \psi \rangle_{\varphi} = \frac{1}{2\pi} \int_{-\pi}^{\pi} d\varphi e^{-i\varphi} \frac{1}{V} \sum_i \frac{1}{m + \lambda_{\varphi}^{(i)}}. \quad (7)$$

In the second step of this equation we have written the chiral condensate as a spectral sum over all eigenvalues  $\lambda_{\varphi}^{(i)}$  of the lattice Dirac operator, computed for boundary angle  $\varphi$ . The mass term is still displayed in this sum, which may be sent to zero after the infinite volume limit is taken. On a finite lattice one of the procedures which we have discussed for the usual chiral condensate has to be applied.

The original motivation for the dual chiral condensate was the idea of constructing an observable which connects the chiral condensate with properties of the Polyakov loop, which in pure  $SU(N)$  gauge theory is an order parameter for the breaking of the center symmetry. The Fourier transform with respect to the boundary angle selects from the closed fermion loops which the chiral condensate consists of, those which have a winding number of one. It is obvious that these loops must transform under center transformations in the same way as the Polyakov loop. An important advantage of the dressed Polyakov loop over the single thin Polyakov loop are its simple renormalization properties which are inherited from the chiral condensate. The Fourier transform allows one to switch between an observable for chiral symmetry breaking to an observable for center symmetry with a simple renormalization.

It is obvious from the definition (7) that the dual chiral condensate can have a non-vanishing value only when the integrand  $I(\varphi) = V^{-1} \sum_i (m + \lambda_{\varphi}^{(i)})^{-1}$  has a non-trivial dependence on the boundary angle  $\varphi$ . In Fig. 9 we show the integrand  $I(\varphi)$  below and above  $T_c$ . Below  $T_c$  it is independent of  $\varphi$  such that we expect a vanishing  $\Sigma_1$  in the deconfined phase. Above  $T_c$  a cosine-like behavior is seen, and the dual chiral condensate is essentially the amplitude of this cosine. It is important to stress that the modulation of  $I(\varphi)$  is not due to the movement of a single eigenvalue, but due to a collective response of the IR part of the spectrum to the changing boundary angle  $\varphi$  [21, 23].

In Fig. 10 we show the results for the dual chiral condensate in physical units and compare it to the behavior of the thin Polyakov loop in lattice units. In the case of a group with non-trivial center both these observables would test

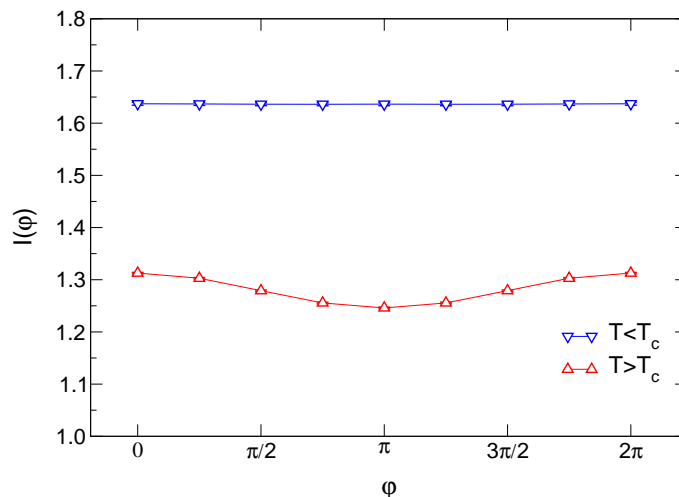


Figure 9: The integrand of the dual chiral condensate at  $am = 0.1$  as a function of the boundary angle  $\varphi$ . We compare the situation below and above  $T_c$ .

for the breaking of center symmetry. Thus in this case qualitatively they should behave the same, i.e., vanish below  $T_c$  and have a finite value above  $T_c$ .

The same behavior is observed also for the case of the center-trivial group  $G_2$ , as is obvious from the figure<sup>3</sup>. For  $G_2$  there is however no simple interpretation in terms of the breaking of the center symmetry - as is the case for the Polyakov loop. It is again remarkable that also  $\Sigma_1$ , which tests for the collective behavior of the IR spectrum as a function of boundary conditions, behaves in the same way as one finds for  $SU(3)$ .

---

<sup>3</sup>We stress that the fact that the data for  $\Sigma_1$  fall on top of the Polyakov loop values is a mere coincidence, since the latter are given in lattice units, and also are subject to large renormalization effects.



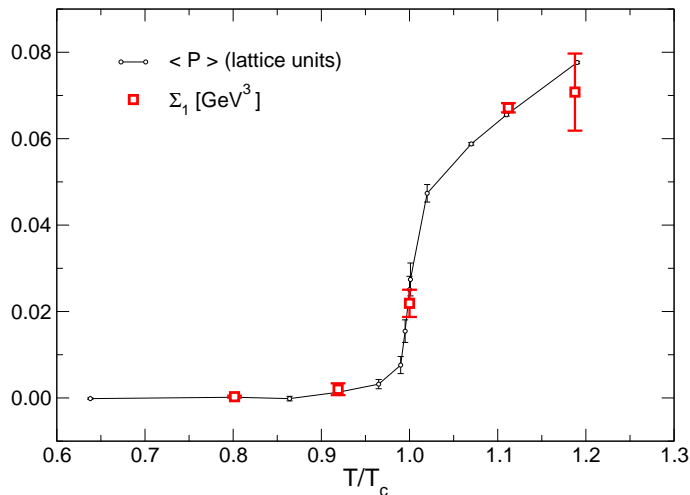


Figure 10: The dual chiral condensate at  $am = 0.1$  (large squares) and the expectation value of the thin Polyakov loop (small circles) as a function of the temperature.

## Concluding remarks

In this article we have analyzed the chiral condensate and spectral properties of the lattice Dirac operator for the center-trivial gauge group  $G_2$ . The study was conducted for quenched gauge configurations at various temperatures below and above  $T_c$ . Varying temporal fermionic boundary conditions were used to probe the system. Of particular interest were the behavior of the chiral condensate and the spectral gap above  $T_c$  for various boundary conditions.

We have demonstrated that chiral symmetry is indeed spontaneously broken. Furthermore, using anti-periodic boundary conditions one finds that the chiral condensate vanishes at exactly the same temperature  $T_c$  where also a thermodynamic transition in the free energy is observed, and which also leaves its trace in the Polyakov loop. In this respect the  $G_2$  gauge theory behaves in the same way as full QCD with fundamental quarks. In addition, we showed that at  $T_c$  a gap opens up in the spectrum as expected from the Banks-Casher formula.

As one switches to periodic boundary conditions the picture changes. The chiral condensate remains finite above  $T_c$  and no gap appears. This is the same behavior as is found for gauge group  $SU(N)$  if the sector with real Polyakov loop is chosen. The other sectors show the same behavior after the fermion boundary

conditions are transformed with a center element of  $SU(N)$ . Above  $T_c$  the spectral gap shows the characteristic sine-type dependence on the boundary angle known from  $SU(N)$ . Finally also the recently proposed dual chiral condensate, which is obtained through a Fourier transformation of the usual condensate with respect to the fermion boundary condition, shows the same behavior as expected from  $SU(N)$ .

Thus we have found that for all spectral and chiral observables which we inspected, the case of gauge group  $G_2$  behaves in exactly the same way as the gauge group  $SU(N)$  when the sector with real Polyakov loop is selected. This is a natural outcome, since the Polyakov loop is always real in  $G_2$ . These results further support the picture that for chiral properties of a theory the sector of the Polyakov loop only acts as a background field with a rather trivial role: For  $G_2$  only a single sector exists and for  $SU(N)$  the results from the different sectors may be mapped onto each other by a suitable transformation of the fermion boundary conditions.

An interesting open puzzle concerning the underlying microscopic mechanism remains: In several papers [2] it was argued that center vortices play a non-trivial role also for the breaking of chiral symmetry. Our finding that in many respects the center-trivial gauge group  $G_2$  produces the same chiral pattern as the real Polyakov loop sector of  $SU(N)$  thus should be understood also from a microscopic point of view. In this respect the proposed domain structure of the  $G_2$  vacuum may be of relevance [6]. This would imply that not the center charge plays a significant role for infrared dynamics, but only the existence of long range structures, as has already been conjectured for gluonic properties [8].

## Acknowledgments

We thank Erek Bilgici, Falk Bruckmann, Christian Hagen, Tamas Kovacs, Christian Lang, Ludovit Liptak, Michael Ilgenfritz, Štefan Olejník, and Uwe Wiese for discussions. The numerical analysis was done at the ZID, University of Graz. J. Danzer is supported by the FWF Doktoratskolleg *Hadrons in Vacuum, Nuclei and Stars* (DK W1203-N08) and C. Gattringer and A. Maas by the FWF Project P20330.

## References

- [1] J. Greensite, Prog. Part. Nucl. Phys. **51** (2003) 1; M. Engelhardt, Nucl. Phys. Proc. Suppl. **140** (2005) 92.

- [2] P. de Forcrand and M. D'Elia, Phys. Rev. Lett. **82** (1999) 4582; J. Gattnar, C. Gattringer, K. Langfeld, H. Reinhardt, A. Schäfer, S. Solbrig and T. Tok, Nucl. Phys. B **716** (2005) 105; PoS **LAT2005** (2006) 301; R. Höllwieser, M. Faber, J. Greensite, U.M. Heller and Š. Olejník, arXiv:0805.1846 [hep-lat]. V.G. Bornyakov, E.M. Ilgenfritz, B.V. Martemyanov, S.M. Morozov, M. Müller-Preussker and A.I. Veselov, Phys. Rev. D **77** (2008) 074507; P. Y. Boyko *et al.*, Nucl. Phys. B **756**, 71 (2006).
- [3] F. Karsch and M. Lutgemeier, Nucl. Phys. B **550** (1999) 449; J. Engels, S. Holtmann and T. Schulze, Nucl. Phys. B **724** (2005) 357.
- [4] K. Holland, P. Minkowski, M. Pepe and U.J. Wiese, Nucl. Phys. B **668**, 207 (2003); Nucl. Phys. Proc. Suppl. **119**, 652 (2003); M. Pepe, PoS **LAT2005** (2006) 017 [Nucl. Phys. Proc. Suppl. **153** (2006) 207].
- [5] M. Pepe and U.J. Wiese, Nucl. Phys. B **768**, 21 (2007).
- [6] J. Greensite, K. Langfeld, Š. Olejník, H. Reinhardt and T. Tok, Phys. Rev. D **75**, 034501 (2007).
- [7] G. Cossu, M. D'Elia, A. Di Giacomo, B. Lucini and C. Pica, JHEP **0710** (2007) 100.
- [8] A. Maas and Š. Olejník, JHEP **0802**, 070 (2008).
- [9] L. Liptak and Š. Olejník, arXiv:0807.1390 [hep-lat].
- [10] E.M. Ilgenfritz, B.V. Martemyanov, M. Müller-Preussker, S. Shcheredin and A.I. Veselov, Phys. Rev. D **66** (2002) 074503; Nucl. Phys. Proc. Suppl. **119** (2003) 754; arXiv:hep-lat/0301008; C. Gattringer *et al.*, Nucl. Phys. Proc. Suppl. **129** (2004) 653; E.M. Ilgenfritz, M. Müller-Preussker and D. Peschka, Phys. Rev. D **71** (2005) 116003.
- [11] C. Gattringer, Phys. Rev. D **67** (2003) 034507; C. Gattringer and R. Pullirsch, Phys. Rev. D **69** (2004) 094510; C. Gattringer and S. Solbrig, Nucl. Phys. Proc. Suppl. **152** (2006) 284.
- [12] C. Gattringer and S. Schaefer, Nucl. Phys. B **654** (2003) 30.
- [13] F. Bruckmann and E.M. Ilgenfritz, Phys. Rev. D **72** (2005) 114502; F. Bruckmann and E.M. Ilgenfritz, PoS **LAT2005** (2006) 305.

- [14] V.G. Bornyakov, E.M. Ilgenfritz, B.V. Martemyanov and M.Müller-Preussker, arXiv:0809.2142 [hep-lat]; V.G. Bornyakov, E.M. Ilgenfritz, B.V. Martemyanov, S.M. Morozov, M.Müller-Preussker and A.I. Veselov, Phys. Rev. D **76** (2007) 054505.
- [15] M.A. Stephanov, Phys. Lett. B **375**, 249 (1996).
- [16] S. Chandrasekharan and N.H. Christ, Nucl. Phys. Proc. Suppl. **47** (1996) 527.
- [17] C. Gattringer, P.E.L. Rakow, A. Schäfer and W. Söldner, Phys. Rev. D **66** (2002) 054502.
- [18] V.G. Bornyakov, E.V. Luschevskaya, S.M. Morozov, M.I. Polikarpov, E.M. Ilgenfritz and M. Müller-Preussker, arXiv:0807.1980 [hep-lat]; PoS **LAT2007** (2007) 315.
- [19] T. Kovacs, PoS **LAT2008** (2008) 198.
- [20] C. Gattringer, Phys. Rev. Lett. **97** (2006) 032003; F. Bruckmann, C. Gattringer and C. Hagen, Phys. Lett. B **647** (2007) 56; C. Hagen, F. Bruckmann, E. Bilgici and C. Gattringer, PoS **LAT2007** (2007) 289; PoS **LAT2008** (2008) 262 [arXiv:0810.0899 [hep-lat]]; E. Bilgici and C. Gattringer, JHEP **0805** (2008) 030.
- [21] E. Bilgici, F. Bruckmann, C. Gattringer and C. Hagen, Phys. Rev. D **77** (2008) 094007.
- [22] W. Söldner, PoS **LAT2007** (2007) 222.
- [23] F. Synatschke, A. Wipf and C. Wozar, Phys. Rev. D **75** (2007) 114003; F. Synatschke, A. Wipf and K. Langfeld, Phys. Rev. D **77** (2008) 114018.
- [24] T.C. Kraan and P. van Baal, Phys. Lett. B **428** (1998) 268; Nucl. Phys. B **533** (1998) 627; Phys. Lett. B **435** (1998) 389; F. Bruckmann and P. van Baal, Nucl. Phys. B **645** (2002) 105.
- [25] M. Garcia Pérez, A. González-Arroyo, C. Pena and P. van Baal, Phys. Rev. D **60** (1999) 031901; M.N. Chernodub, T.C. Kraan and P. van Baal, Nucl. Phys. Proc. Suppl. **83** (2000) 556.
- [26] T. Banks and A. Casher, Nucl. Phys. B **169** (1980) 103.
- [27] A. Maas, Mod. Phys. Lett. A **20** (2005) 1797.